UNIVERSITY of CALIFORNIA
SANTA CRUZ

THERMAL EVOLUTION OF URANUS AND NEPTUNE WITH CONDENSATION-INHIBITED CONVECTION

A thesis submitted in partial satisfaction of the
requirements for the degree of

BACHELOR OF SCIENCE

in

ASTROPHYSICS

by

Robert Schroder

November 2020

Abstract

Thermal Evolution of Uranus and Neptune with Condensation-inhibited Convection

by

Robert Schroder

This will be the last section written, once we have finished our results and conclusion.

Contents

List of Figures

List of Tables

To Who,

M ention to who, if anyone, here

Acknowledgements

I'd like to think....

1

Introduction

Observations of Uranus show a planet that appears to be in thermal equilibrium with the Sun. Observation has also shown that Uranus is cooler than its more distant neighbor, Neptune. Thermal evolution models for Uranus have not matched observation, instead predicting a warmer effective temperature during the current epoch(Fortney et al., 2011), (M. Podolak, 1991), (W.B. Hubbard, 1995), (L. Scheibe, 2019) [There are other papers by Nettelmann 2013, Linder 2019 that I haven't looked at yet].

There have been various attempts to explain the underluminous Uranus. The formation of stable layers, trapping internal energy in the the interior of Uranus and Neptune was proposed by (M. Podolak, 1991). There has also been much work done investigating the formation of stable condensation zones that inhibit convection (Friedson & Gonzales, 2017), (Leconte et al., 2017), and (Guillot, 1995).

2

Model

2.1 Theoretical Foundations for Fully Convective, Dry Interior

Underlying the model are mathematics and physics dating back to the first attempts to model the thermal evolution of giant planets (Hubbard, 1977b) and later attempts to model Uranus and Neptune (Hubbard, 1977a) and (M. Podolak, 1991). We begin with conservation of mass:

$$\frac{dm}{dr} = 4\pi r^2 \rho \tag{2.1}$$

where dm is the mass contained within a sphere of radius r. $\rho(r)$ is the density at radius r. We also assume hydrostatic equilibrium, given by:

$$\frac{dP}{dr} = -\frac{Gm\rho}{r^2} \tag{2.2}$$

where P is the pressure and G is the gravitational constant. For onservation of energy and the thermal evolution of the planet, we relate the intrinsic luminosity profile $L(m)$ to the rate of change of specific entropy s in the planet as follows:

$$\frac{dL}{dm} = -T\frac{\delta s}{\delta t}. \tag{2.3}$$

Integrating over the mass of the planet and solving for the timestep, δt, yields

$$\delta t = -\frac{1}{L_{\text{int}}}\int_0^M T\,\delta s\,dm \tag{2.4}$$

where L_{int} is the intrinsic luminosity, given by:

$$L_{\text{int}} = 4\pi r^2 \sigma_{\text{SB}} T_{\text{int}}^4 \tag{2.5}$$

Furthermore, for our base comparison model, we assume a standard three-layer structure for Uranus and Neptune as seen in Figure 2.1. At the center of the planet is a core made of ??. The inner envelope is H_2O dominated, with uniform concentrations of H, He, and H_2O, using the MAZEVET EOS (S. Mazevet & Potekhin, 2019). The outer envelope, below 10 bars, contains trace amounts of H_2O, but is mostly H and He, dominated, and utilizes the MH13SCVH EOS (Y. Miguel & Fayon, 2018). Both inner and outer envelopes are fully convective, with the pressure-temperature profile following a dry adiabat, given by ∇_{ad}:

$$T(P > P_{\text{base}}) = T_{\text{base}} + \int_{P_{\text{base}}}^{P} \left(\frac{dT}{dP}\right)_{\text{ad}} dP \tag{2.6}$$

Finally, beyond the outer envelope is the atmosphere. When modeling the thermal evolution of gas and ice giants, it has long been recognized that model atmospheres

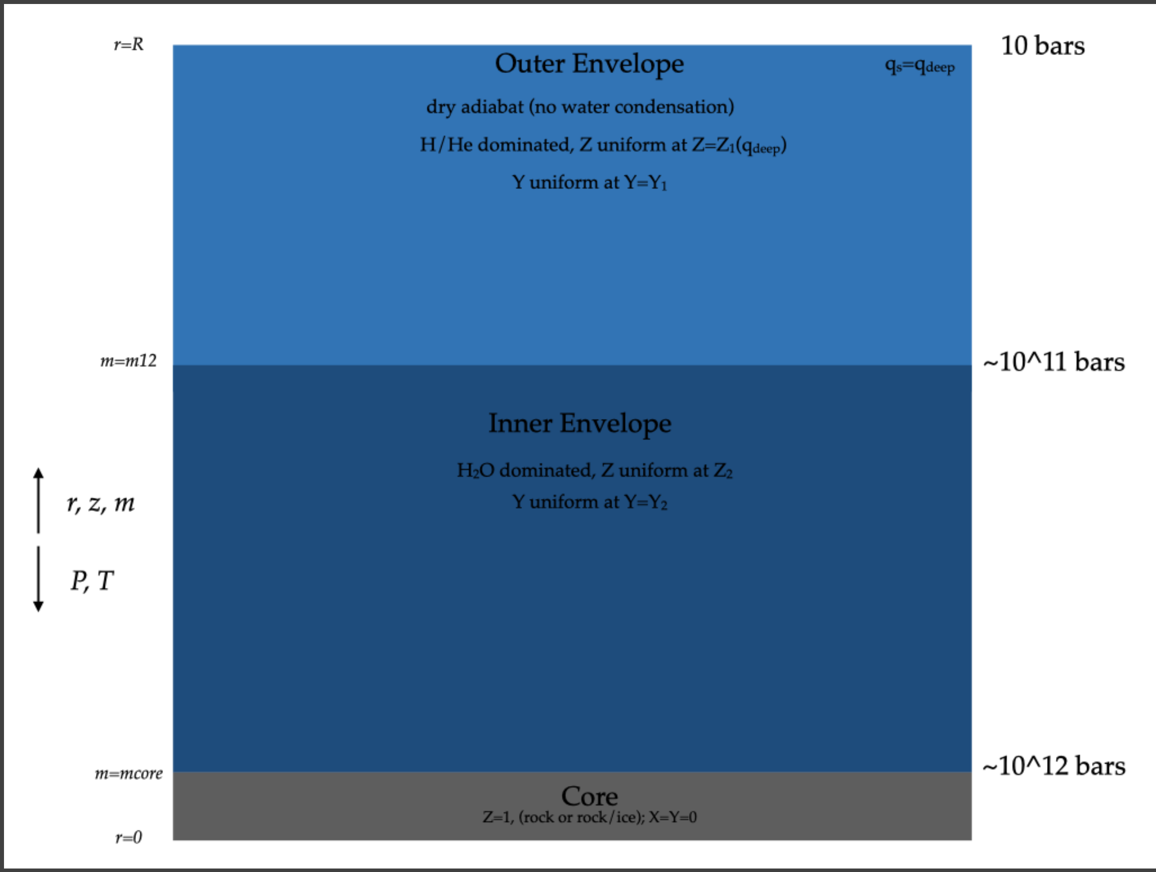

Figure 2.1: The structure for a fully convective, dry adiabatic interior.

constitute an outer boundary condition for interior structure models, providing key inputs that impact cooling times for interior structure models. Our work considers both (Harold C. Graboske & Olness, 1975) and (Fortney et al., 2011) model atmospheres. Unless otherwise stated, our results will utilize the Fortney 2011 model atmospheres.

2.2 Addition of a Moist Adiabat to the Outer Envelope with Condensation-inhibited Convection

Our interior structure model departs from the standard model described above by adding a moist adiabatic layer to the outer envelope. In our case, this allows for the condensation of water. We do not account for other condensates such as CH_4 and NH_3.

As seen in Figure (Y). Within the outer envelope, we implement moist adiabatic layer, such that when conditions are suitable for condensation, we allow for the formation of a stable water condensation zone. ADD PHYSICS FOR CONDENSATION (Include equations for q_s, latent heat, xi, saturation vapor pressure, ... other equations that define the moist adiabat.)

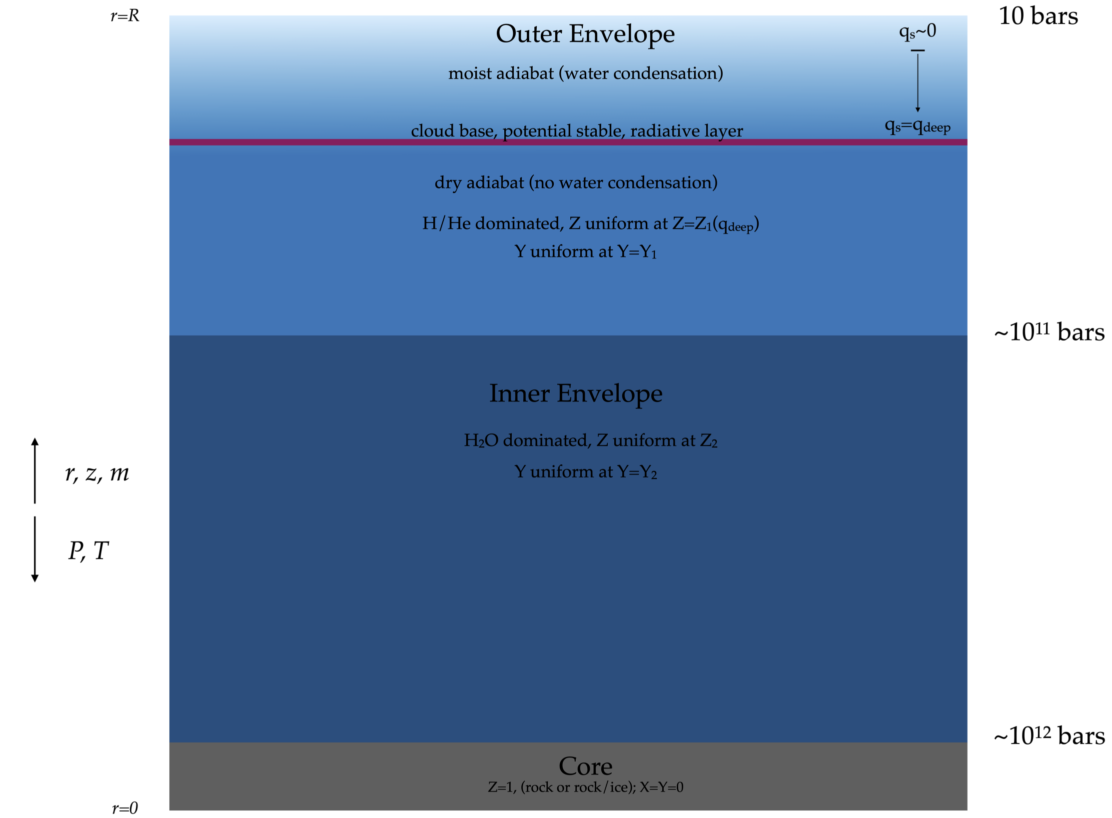

Figure 2.2: The structure for moist adiabatic interior, allowing for condensation-inhibited convection.

If condensation zone forms, it may be stable against convection. Convection is inhibited due to the formation of a stable condensation zone when $\alpha < 1$, where is α

(Friedson & Gonzales, 2017) is given by:

$$\alpha = 1 + \xi(q_s L / R_W T_0) \tag{2.7}$$

If condensation is found to be inhibited,

At pressure where $\alpha < 1$, the cloud base of the water condensation zone forms. This thin, stable radiative layer has a temperature profile that is governed by:

$$T(P) = T_{\text{top}} + \int_{P_{\text{top}}}^{P} \left(\frac{dT}{dP}\right)_{\text{rad}} dP \tag{2.8}$$

$$\left(\frac{dT}{dP}\right)_{\text{rad}} = \frac{T}{P}\nabla_{\text{rad}} = \frac{T}{P} \times \frac{3}{16}\frac{\kappa_R P}{g}\frac{T_{\text{int}}^4}{T^4} \tag{2.9}$$

$$T_{\text{base}} \equiv T(P + \Delta P) = T_{\text{top}} + \left(\frac{dT}{dP}\right)_{\text{rad}} \Delta P. \tag{2.10}$$

$$x_{\text{vap}}(P,T) = x_{\text{vap}}^{\text{sat}}(P,T) = \frac{e_s(T)}{P}, \qquad P < P_{\text{base}}. \tag{2.11}$$

$$x_{\text{vap}}^{\text{sat}}(P_{\text{base}}, T_{\text{base}}) = \frac{e_s(T_{\text{base}})}{P_{\text{base}}} = x_{\text{vap}}^{\text{deep}} \Longrightarrow \Delta P \equiv P_{\text{base}} - P_{\text{top}} = \frac{e_s(T_{\text{base}})}{x_{\text{vap}}^{\text{deep}}} - P_{\text{top}} \tag{2.12}$$

$$T_{\text{base}} = T_{\text{top}} + \left(\frac{dT}{dP}\right)_{\text{rad}} \left(\frac{e_s(T_{\text{base}})}{x_{\text{vap}}^{\text{deep}}} - P_{\text{top}}\right) \tag{2.13}$$

Below the base of the radiative layer, the temperature-pressure profile again follows a dry adiabat, given by Equation (2.1).

3

Results

3.1 Condensation-inhibited Convection

Talk about Figure 3.1.

3.2 Formation of Radiative Layer

Talk about Figure 3.2.

3.3 Thermal Evolution

Talk about Figure 3.3.

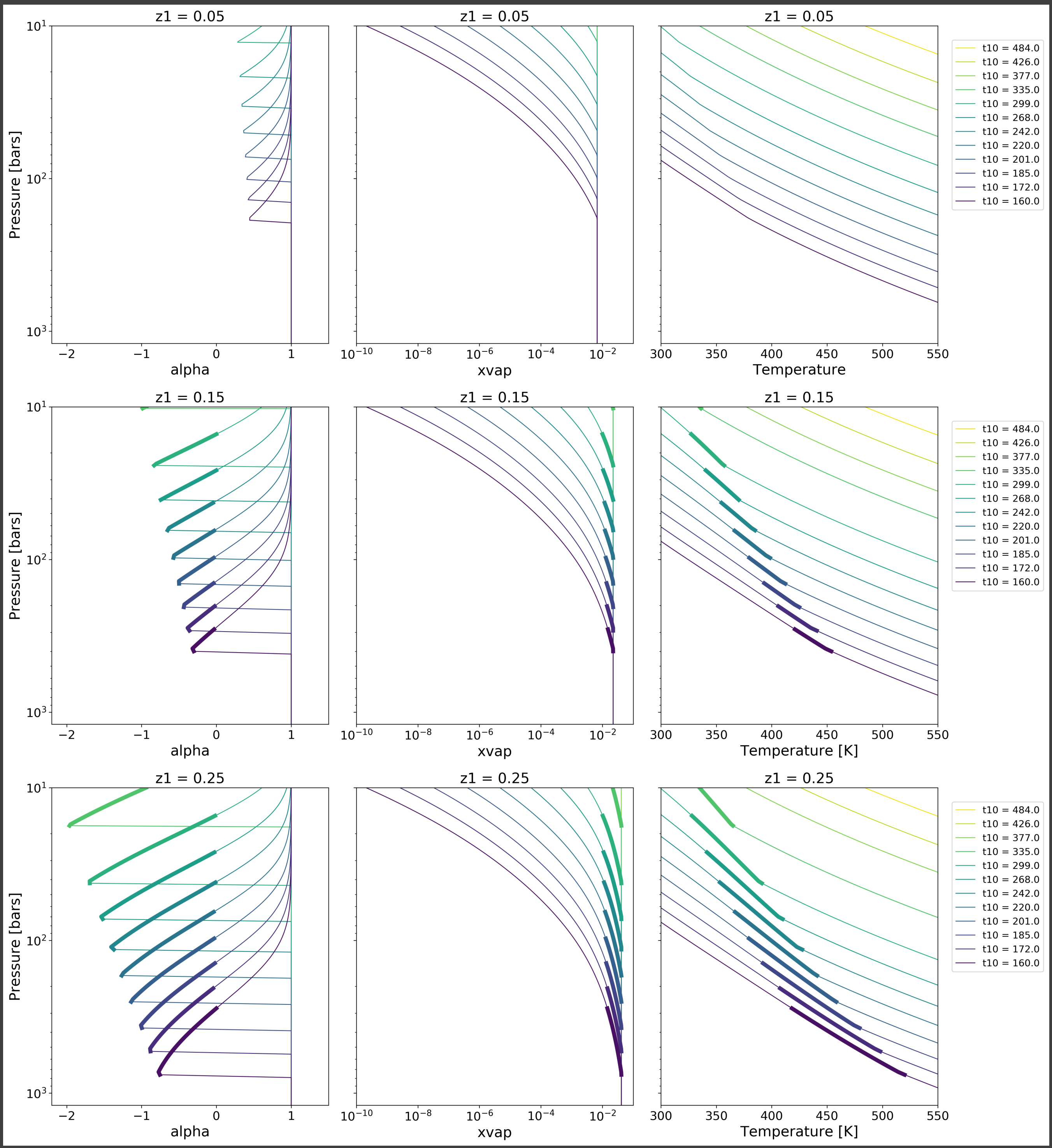

Figure 3.1: add description re: moist adiabat, when/where convection is inhibited and where the radiative zone base is in these plots. explain differences

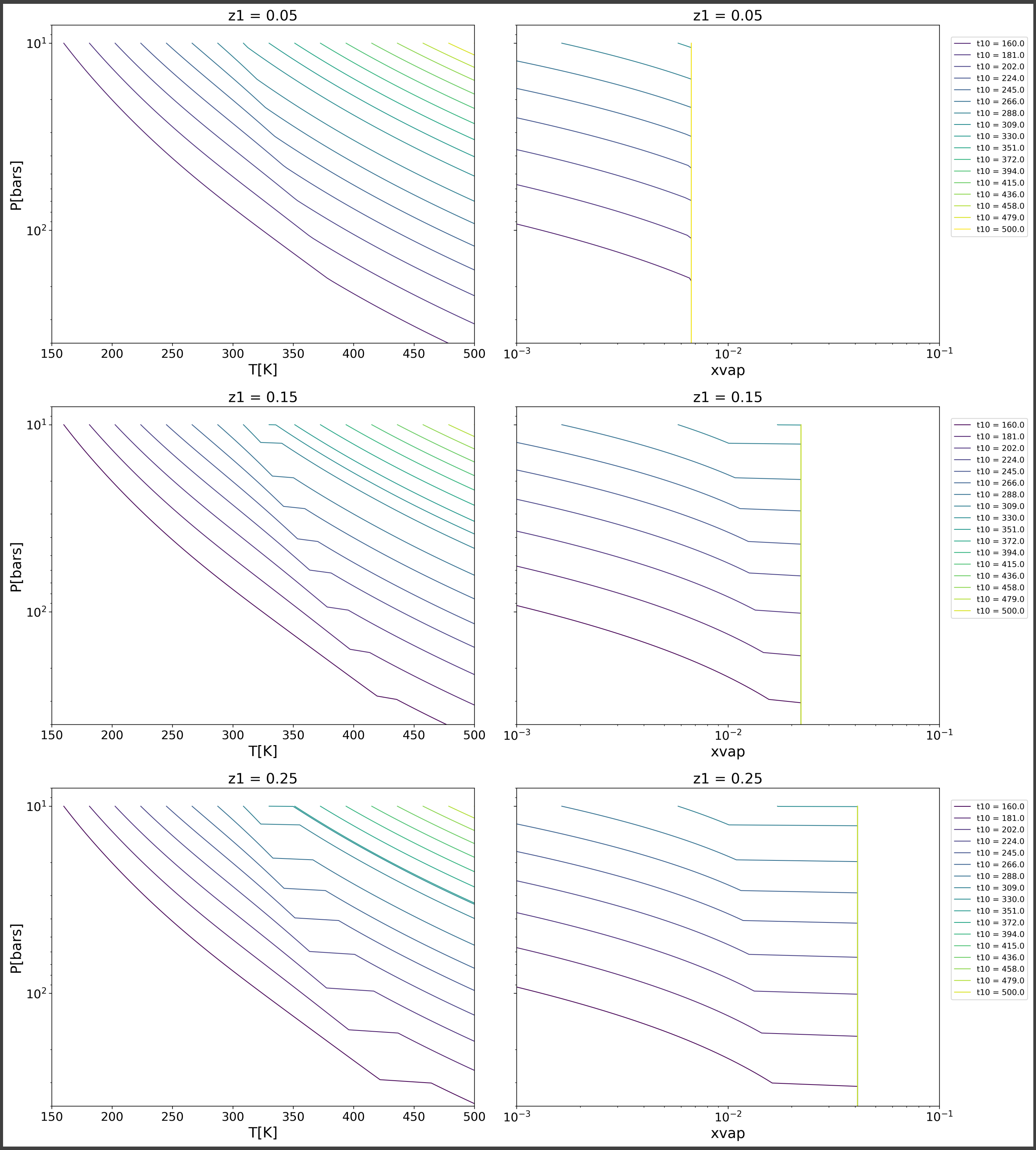

Figure 3.2: add description these plots. explain differences

4

Discussion and Conclusions

Appendix A

Some Ancillary Stuff

Bibliography

Fortney, J. J., Ikoma, M., Nettelmann, N., Guillot, T., & Marley, M. S. (2011). Self-consistent model atmospheres and the cooling of the solar system's giant planets. *The Astrophysical Journal*, 729, 32.

Friedson, A. J. & Gonzales, E. J. (2017). Inhibition of ordinary and diffusive convection in the water condensation zone of the ice giants and implications for their thermal evolution. *Icarus*, 297, 160–178.

Guillot, T. (1995). Condensation of methane, ammonia, and water and the inhibition of convection in giant planets. *Science*, (pp. 1697–1699).

Harold C. Graboske, Jr., J. B. P. A. S. G. & Olness, R. J. (1975). The structure and evolution of jupiter: The fluid contraction. *The Astrophysical Journal*, 199, 265–281.

Hubbard, W. (1977a). Comparative thermal evolution of uranus and neptune. *Icarus*, , 35, 177–181.

Hubbard, W. (1977b). The jovian surface condition and cooling rate. *Icarus*, , 30, 305–310.

L. Scheibe, N Nettelmann, R. R. (2019). Thermal evolution of uranus and neptune: Adiabatic models. *Astronomy and Astrophysics*, A70, 632.

Leconte, J., Selsis, F., Hersant, F., & Guillot, T. (2017). Condensation-inhibited convection in hydrogen-rich atmospheres: Stability against double-diffusive processes and thermal profiles for jupiter, saturn, uranus, and neptune. *Astronomy and Astrophysics*, A98, 598.

M. Podolak, W.B. Hubbard, D. S. (1991). Models of uranus' interior and magnetic field. *Uranus, Editors: J.T. Bergstralh, E.D. Miner, M. Shapely Matthews*, (pp.$\tilde{2}$9).

S. Mazevet, A. Licari, G. C. & Potekhin, A. Y. (2019). Ab initio based equation of state of dense water for planetary and exoplanetary modeling. *Astronomy & Astrophysics*, A128, 621.

W.B. Hubbard, D. S. (1995). The interior of neptune. *Neptune and Triton, Editor: D.P. Kruikshank*, (pp. 109).

Y. Miguel, T. G. & Fayon, L. (2018). Jupiter internal structure: the effect of different equations of state. *Astronomy & Astrophysics*, C2, 618.